  Bull. Chem. Soc. Jpn., 59, 1425—1431 (1986)

Studies of Liquid Water by Computer Simulations. IV. Transport Properties of a 2-D Model

Yosuke KATAOKA
Department of Chemistry, Faculty of Science, Kyoto University, Kyoto 606
(Received September 5, 1985)

The constant-temperature constant-pressure molecular dynamics simulations of a water-like system are performed at many temperatures and pressures. A 2-dimensional model of water is used for the system with 576 molecules in a square cell. Thermodynamical quantities are anomalous as in liquid water. The temperature-dependences of the calculated self-diffusion coefficient and the shear viscosity are in agreement with the observed values at low pressures. The effects of compression on these transport coefficients are reproduced qualitatively. The bulk viscosity obtained is larger than the shear viscosity. The order of magnitude of the calculated thermal conductivity is in agreement with the experimental results. The contribution of the rotational motion to the thermal conductivity is calculated in order to discuss the anomalous temperature-dependence of this coefficient.

The behavior of the shear viscosity[1-6] and the self-diffusion coefficient[7-11] of liquid water at temperatures below about 300 K is unique. The initial application of pressure causes the viscosity to decrease, and the diffusion coefficient to increase. The Stokes-Einstein equation is valid even in supercooled water.[4-5] Although there are some molecular dynamics(MD) calculations of the self-diffusion coefficient,[12-14] it seems that a systematic study has not yet been performed on the viscosity nor on the thermal conductivity. The thermal conductivity of liquid water has a maximum as a function of temperature under constant pressure.[2,15,16] The thermal conductivity has considerable technical importance, but our understanding of the molecular behavior underlying the phenomenon is poorly developed.[2] Only a couple of phenomenological theories has been published concerning the anomaly of the thermal conductivity.[17,18] For this reason, we are planning to perform MD simulations at many temperatures and pressures to obtain the transport coefficients of liquid water.

Since the calculation of the transport coefficients is not easy,[19-22] we use the 2-D model of water,[23] as the first step. Despite theoretical predictions that transport coefficients in 2-D system diverge, a computer simulation of the small system can be used to study the transport properties.[24-27]

In the first paper of this series,[23] it was shown that a simple 2-D model of water can reproduce the main features of the thermodynamical behavior observed in real water. In the previous article,[28] dynamical properties of the 2-D water were studied by microcanonical MD simulation. The dipole direction relaxation time and the self-diffusion coefficient were calculated as functions of temperature and density. The effects of compression on these quantities are in good agreement with the experimental data.[28]

We use constant temperature and constant pressure MD(*T-P*-MD), because this method is more convenient to obtain the temperature dependence or pressure dependence of the system. Many methods are developed for the constant temperature MD.[29-34] Among them, Nosé's method[34] is used because this can conveniently be combined with Andersen's constant pressure MD.[31] By *T-P*-MD, the isothermal compressibility, the thermal expansion coefficient and the heat capacity at constant pressure are calculated from the fluctuations of the relevant quantities. Transport coefficients are calculated using the standard Kubo formula.[36]

As we have no experimental results on any 2-D water-like liquid, the absolute values obtained will be compared with those of the real water, where we shall use reduced units.[23] In the qualitative comparison of the temperature and pressure dependences, arbitrary scales will be used as follows.

The zero point of the thermal expansion coefficient and its maximum near the critical temperature are used to fix the temperature scale tentatively for the comparison of the calculated results with those of real water. By such a comparison, it is shown that the calculated transport coefficients are in agreement with those of real water. Although the maximum of the thermal conductivity as a function of temperature is not obtained, it is found that the contribution of the rotational motion to this coefficient has a maximum.

Molecular Dynamics Method

The 2-D model of water has been described in the first paper of this series.[23] The micro canonical molecular dynamics calculation was performed previously.[28] Therefore only the new aspects are described here.

The mass M of the molecule is 18 in units of atomic weight and the moment of inertia I is 3.34×10^{-44} gm^2. We use the following reduced units.[28] The energy E is measured in units of ε_0=24.68 kJ mol^{-1}($-\varepsilon_0$ is the absolute minimum of the

pair potential energy), the temperature in units of ε_0/k_B (k_B is the Boltzmann constant), the length in units of R_0=0.276 nm. The unit of time is

$$t_0 = (MR_0^2/\varepsilon_0)^{1/2} = 2.37\times 10^{-13}\ \mathrm{s}. \quad (1)$$

The system consists of 576 molecules in a square unit cell with the periodic boundary condition. The dynamical equations are integrated with time increment

$$\Delta t = 0.435\times 10^{-15}\ \mathrm{s} = 0.00184\, t_0 \quad (2)$$

by the predictor-corrector method.[37,38]

The constant temperature MD method of Nośe[34] is used in this paper. According to Nośe,[34] an additional degree of freedom s is introduced which acts as an external system on the system of N molecules. A constant Q appears in the kinetic energy part as $p_s^2/2Q$ in the total Hamiltonian, where p_s is the conjugate momentum of s. After some trial and error calculations, we have decided somewhat arbitrarily to choose 636 $\varepsilon_0 t_0^2$ for Q. The constant pressure MD method of Andersen is combined. In this method, the area A of the N molecular system is a variable. A constant W is introduced in the kinetic term as $p_A^2/2W$ where p_A is the conjugate momentum of A. We chose $1.92\times 10^{-3}\ \varepsilon_0 t_0^2$ as the value of W after some preliminary simulations.

The total energy is conserved within 0.02% after 60000 steps, or 26 ps. In our standard run, 60000 steps are spent for the aging of the system. After this interval, the 60000-step run is performed at least twice, where the molecular dynamics statistical averages are obtained.

The shear viscosity, the bulk viscosity and the thermal conductivity are calculated by the standard Kubo type formula.[19,36] Averages of at least 6000 values are taken for the initial time in the standard 60000-step run. Some long runs are needed at low temperatures because of the long tail of the correlation function for the shear viscosity. In such cases, the MD run is as long as 120000 steps. The representative range of the time integration of the correlation function for the shear viscosity is $0\leq t\leq 3.6$ ps at T=0.194 ε_0/k_B, P=0.186 ε_0/R_0^2.

Thermodynamical Properties

The thermodynamic coefficients such as the thermal expansion coefficient, the isothermal compressibility and the heat capacity at constant pressure are easy to calculate because of the constant temperature and constant pressure MD method used in this paper. First the calculated thermodynamical quantities are compared with the experimental results. The temperature scale for the comparison is shown in this section. It will be used also in the comparison of the transport coefficients in the next section.

The thermal expansion coefficient at constant pressure, α, is calculated from the cross fluctuation of area A and enthapy H[35] (circle in Fig. 1)

$$\alpha = \frac{\langle AH\rangle - \langle A\rangle\langle H\rangle}{k_B T^2 \langle A\rangle}, \quad (3)$$

and also from the numerical differentiation of the area A of the N-molecule system (triangle in Fig. 1). The pressure P=0.186 ε_0/R_0^2 in Fig. 1 is the representative low pressure in 2-D water.[23] The results by these methods are in good agreement with the experimental values[1,2,39,40] if we use the temperature scale shown in Fig. 1. (The temperature scale for real water is shown in the upper part. The zero point and the scale of temperature for the real water are different from those for 2-D water. For this reason, the comparisons of the temperature dependences are only qualitative in the following figures.) In this figure, the experimental results are shown by the dotted line (normal pressure) and the dash-dotted line (P=100 MPa). As for the absolute value of the calculated expansion coefficient, the comparison is satisfactory at moderate temperatures. The coefficient obtained around the critical temperature T_c is small compared with the experimental results. This may result from the small number of molecules in the basic cell (N=576). The critical temperature of our 2-D water is about 0.263 ε_0/k_B and the critical pressure P_c is about 0.17 ε_0/R_0^2 which were estimated by the equation of state.[23]

The isothermal compressibility κ_T is calculated from the fluctuation[35] as shown below (triangle in

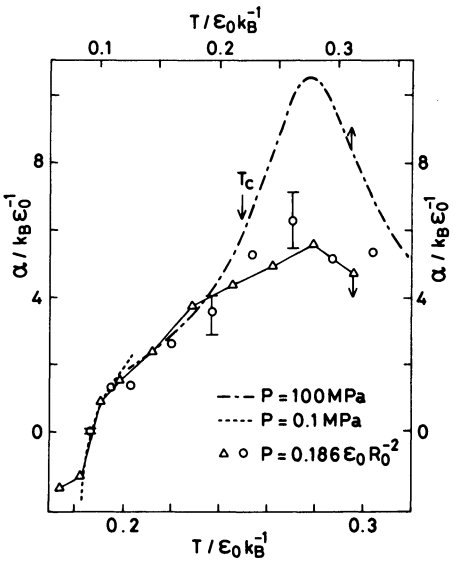

Fig. 1. Plot of the thermal expansion coefficient α vs. temperature T, at P=0.186 ε_0/R_0^2, ○ from the fluctuation, △ from the differentiation of the area. The dotted and the dash-dotted lines show the experimental results.[1,2,39,40]

Fig. 2):

$$\kappa_T = \frac{\langle A^2\rangle - \langle A\rangle^2}{k_B T\langle A\rangle}, \tag{4}$$

and by means of the radial distribution function $g(R)$[35] (circle in Fig. 2)

$$\kappa_T = \frac{\langle A\rangle}{k_B TN} + \frac{1}{k_B T}\int_0^\infty [g(R)-1]2\pi R dR. \tag{5}$$

The results are in agreement with the experimental ones.[1,2,40,41] We can see that the calculated compressibility has a reasonable value at moderate temperatures, and that the anomalies at low temperatures and at high temperatures are reproduced at least qualitatively.

The calculated heat capacity at constant pressure, C_p, is shown in Fig. 3, where the circles are the values

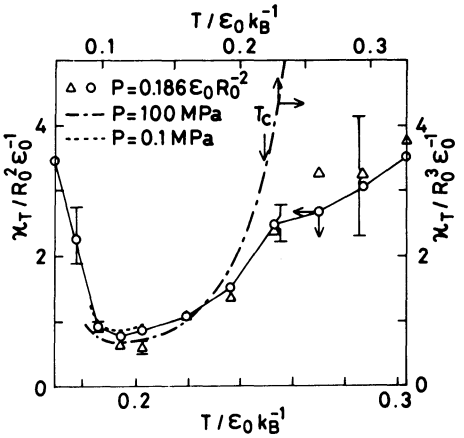

Fig. 2. Plot of the isothermal compressibility κ_T vs. temperature T, at $P=0.186\ \varepsilon_0/R_0^2$, △ from the fluctuation, ○ from the radial distribution function. The dotted and the dash-dotted lines show the experimental results.[1,2,40,41]

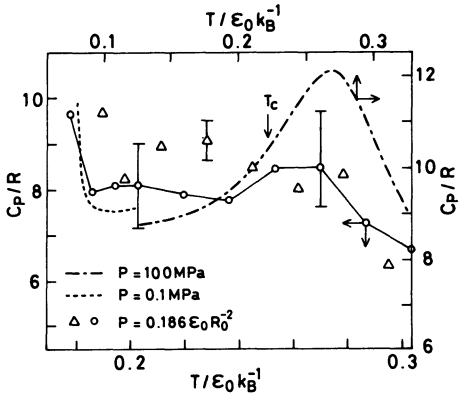

Fig. 3. Plot of the heat capacity at constant pressure C_p vs. temperature T, at $P=0.186\ \varepsilon_0/R_0^2$, ○ from the fluctuation, △ from the differentiation of H. The dotted and the dash-dotted lines show the experimental results.[1,2,40,42]

obtained from the fluctuation of the enthalpy H

$$C_p = \frac{\langle H^2\rangle - \langle H\rangle^2}{k_B T^2}, \tag{6}$$

and the triangles mean the result of the numerical differentiation of the enthalpy with respect to temperature. Unfortunately the calculated results scatter. We see however that the absolute values are in agreement with the experimental results. The temperature dependence is not inconsistent with that of the experimental values.[1,2,40,42]

Transport Coefficients

In this section, the calculated transport coefficients are compared with the experimental results and the time correlation functions are discussed.

The self-diffusion coefficient D is calculated from the mean square displacement $\langle\Delta r^2\rangle$ and from the velocity auto-correlation function.[38]

$$D = \lim_{t\to\infty}\frac{\langle\Delta r^2\rangle}{4t}, \tag{7}$$

$$D = \frac{1}{2}\int_0^\infty \langle v(t)\cdot v(0)\rangle dt. \tag{8}$$

The calculated coefficient D is plotted against pressure in Fig. 4 for several temperatures. The experimental results are shown by the dotted lines.[7-11] The anomaly of the self-diffusion coefficient is qualitatively reproduced as shown in Fig. 4 if we tentatively use the pressure scale for comparison with real water. The pressure scales and zero points are arbitrary for the purpose of qualitative comparison in Figs. 4 and 7.

The shear viscosity η and the bulk viscosity η_B are calculated from the relevant time correlation functions:[19,36]

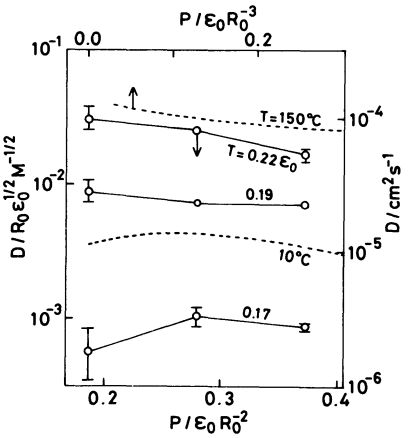

Fig. 4. Plot of the self-diffusion coefficient D vs. pressure P. Values of the temperature are indicated next to each curve.
The dotted lines are the experimental results.[7-11]

$$\eta = \frac{1}{k_B T\langle A\rangle}\int_0^\infty \langle J^{xy}(t)\cdot J^{xy}(0)\rangle \mathrm{d}t, \tag{9}$$

$$\eta_B = \frac{1}{4k_B T\langle A\rangle} \times \sum_{\alpha,\beta=x,y}\int_0^\infty \langle [J^{\alpha\alpha}(t)-\langle J^{\alpha\alpha}\rangle]\cdot[J^{\beta\beta}(0)-\langle J^{\beta\beta}\rangle]\mathrm{d}t, \tag{10}$$

$$J^{\alpha\beta} \equiv M\sum_i v_{i\alpha}v_{i\beta} + \sum_i r_{i\alpha}f_{i\beta}, \tag{11}$$

where M is the mass of the molecule and $v_{i\alpha}$ the α component of the velocity of i-th molecule. And r_i means the position of the i-th molecule and f_i is the force that the i-th molecule feels.

The viscosities obtained are shown in Fig. 5, where the results by several MD methods are compared. In this figure each circle (shear viscosity) and triangle (bulk vicosity) means the value obtained from each 60000-step run. The bar shows the average. Although the calculated values scatter, the shear viscosity can be obtained by the constant temperature and constant pressure MD (T-P-MD) as shown in this figure. Contrary to this, the orders of magnitude of the bulk viscosity by P-MD and T-P-MD were different from that of bulk viscosity by the micro canonical MD. This may arise from the fact that the bulk viscosity is related to the fluctuation of pressure P (see Eq. 10) and the area A is controlled in P-MD so the time dependence of P is artificial in this special MD.

Figure 5 shows that the bulk viscosity η_B is larger than the shear viscosity (at T=0.194 ε_0/k_B, P=0.186 ε_0/R_0^2):

$$\frac{\eta_B}{\eta} = 1.4 \tag{12}$$

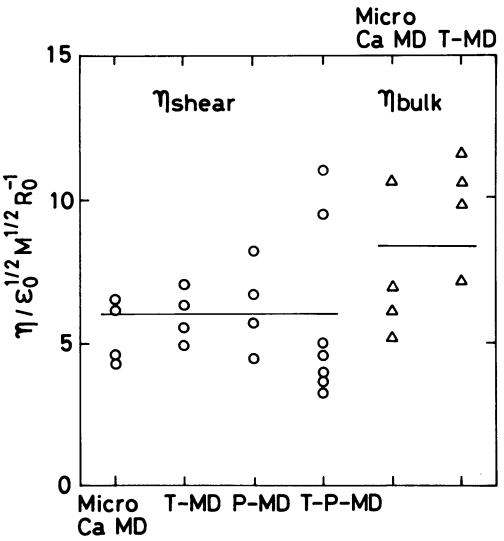

Fig. 5. Shear viscosity (○) and bulk viscosity (△) by several MD methods at T=0.194 ε_0/k_B, P=0.186 ε_0/R_0^2.

in accordance with the experimental results.[2,43] This feature is confirmed at another state (T=0.186 ε_0/k_B, P=0.216 ε_0/R_0^2), where the value of the ratio is also η_B/η=1.4.

The temperature dependence of the shear viscosity η at P=0.186 ε_0/R_0^2 is shown in Fig. 6, where the temperature scale is the same as that in Fig. 1. We see that the shear viscosity in the reduced units has a reasonable value as a function of temperature in Fig. 6. The calculated shear viscosity η is plotted against pressure P at several temperatures in Fig. 7. The experimental results are shown in the dotted lines.[1,6] The main anomalous feature in the shear viscosity of liquid water is seen in Fig. 7.

The shear viscosity η and the self-diffusion co-

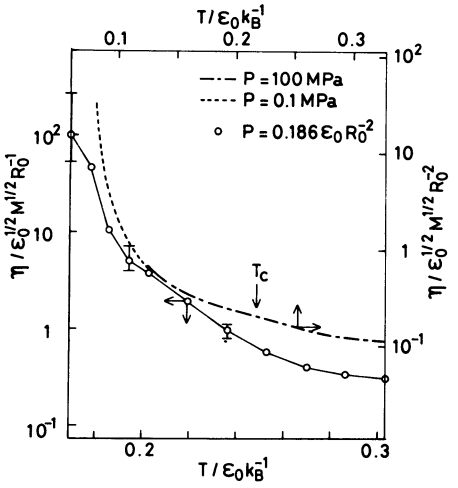

Fig. 6. Plot of the shear viscosity η vs. temperature T, at P=0.186 ε_0/R_0^2.
The dotted and the dash-dotted lines show the experimental results.[1-6]

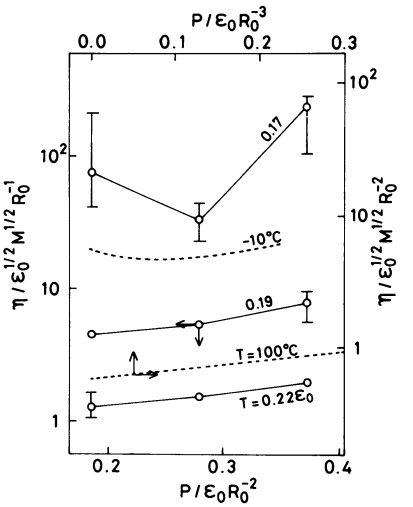

Fig. 7. Plot of the shear viscosity η vs. pressure P. Values of the temperature are indicated next to each curve.
The dotted lines are the experimental results.[1-6]

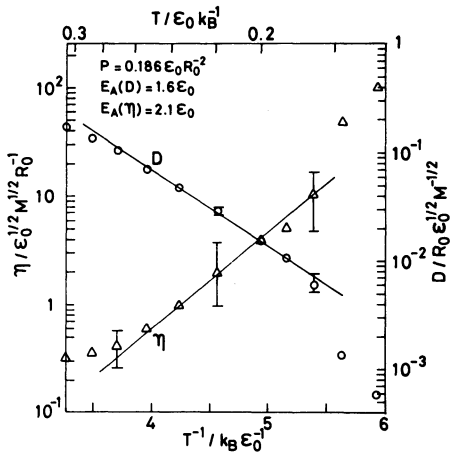

Fig. 8. Shear viscosity η and self-diffusion coefficient D vs. $1/T$ at $P=0.186\ \varepsilon_0/R_0^2$.

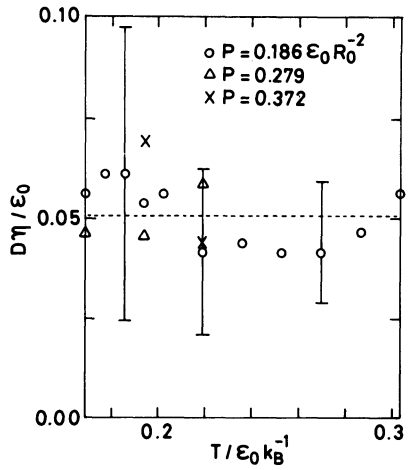

Fig. 9. Plot of the product ηD vs. T.

efficent D are plotted against $1/T$ in Fig. 8. As shown in this figture these quantities have about the same activation energy, so the product of these ηD is almost constant as a function of temperature as shown Fig. 9.

The thermal conductivity λ is calculated by the correlation function of the heat current $S(t)$:

$$\lambda = \frac{1}{2k_B T^2 \langle A \rangle} \int_0^\infty \langle \boldsymbol{S}(t) \cdot \boldsymbol{S}(0) \rangle dt, \tag{13}$$

$$\boldsymbol{S}(t) \equiv \frac{d}{dt} \sum_i H_i \boldsymbol{r}_i, \tag{14}$$

were H_i is the contribution of the i-th molecule to the total Hamiltonian of the system $\mathscr{H}$:

$$\mathscr{H} = \sum_i H_i. \tag{15}$$

The calculated thermal conductivity λ is shown in Fig. 10 (open circle). The dotted line corresponds to the observed value at normal pressure.[2,15,16] The dash-dotted line means the experimental conductivity

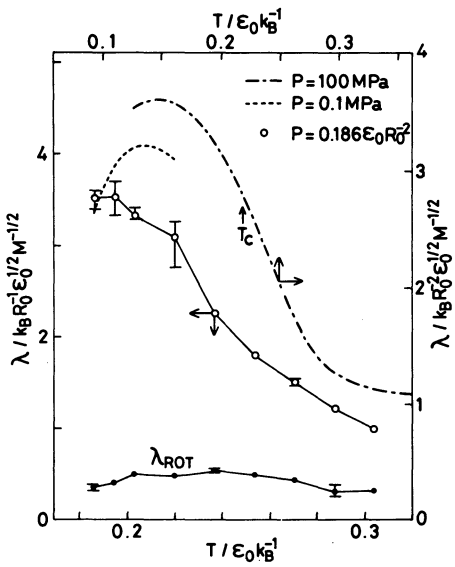

Fig. 10. Plot of the thermal conductivity λ vs. temperature T at $P=0.186\ \varepsilon_0/R_0^2$ (○).
The contribution from the rotational motion is also shown (●). The dotted and the dash-dotted lines show the experimental results.[2,15,16,44]

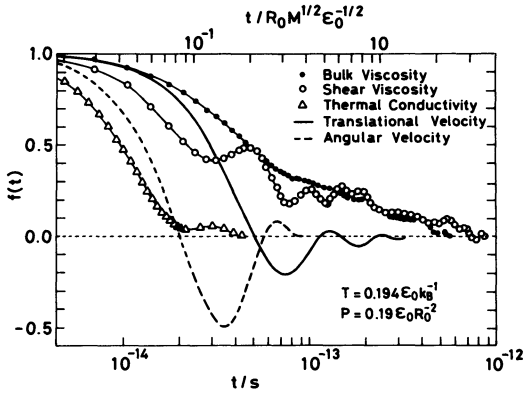

Fig. 11. The normalized correlation functions for the transport coefficients $f(t)$ vs. time t, at $T=0.194\ \varepsilon_0/k_B$, $P=0.186\ \varepsilon_0/R_0^2$.

under pressure (P=100 MPa)[44] in this figure.

The order of magnitude of the calculated thermal conductivity is in agreement with those of the experimental results if we use the reduced quantities. The conductivity obtained has a tendency to saturate when the temperature is decreased. However, the maximum is not seen in the calculated temperature dependence of the conductivity. The contribution of the rotational motion is also shown in this figure (closed circle). This part has a maximum as a function of temperature. This contribution comes from the differentiation of the molecular Hamiltonian H_i with respect to the angle of the molecule φ:

$$\frac{dH_i}{dt} = \sum_j \left[\frac{\partial H_i}{\partial x_j} \dot{x}_j + \frac{\partial H_i}{\partial y_j} \dot{y}_j + \frac{\partial H_i}{\partial \varphi_j} \dot{\varphi}_j \right]. \tag{16}$$

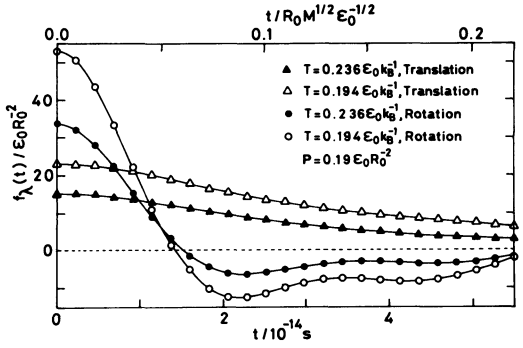

Fig. 12. The unnormalized correlation functions for the thermal conductivity $f_\lambda(t)$ vs. time t, at $P=0.186$ ε_0/R_0^2.

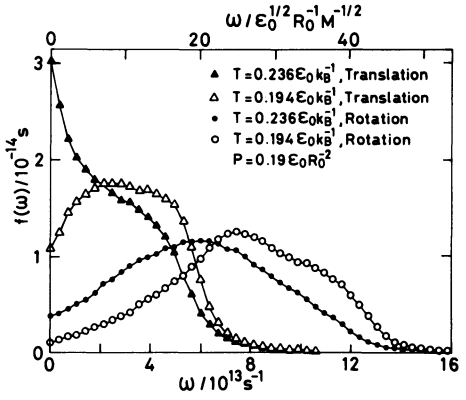

Fig. 13. The Fourier transforms of the correlation functions of velocity at $P=0.186$ ε_0/R_0^2.

We expect such a contribution is more important in real water than in 2-D water which has only one rotational degree of freedom.

The normalized correlation functions are shown in Fig. 11 in order to see the microscopic aspects of the transport coefficients (cf Ref. 19). The long tails are seen in the correlation functions for the shear viscosity (open circle) and bulk viscosity (closed circle). In contrast to these, the correlation function for the thermal conductivity has a short tail at this state ($T=0.194$ ε_0/k_B, $P=0.186$ ε_0/R_0^2). Its correlation time is about the same with as that of the correlation function of the rotational velocity.

The non-normalized correlation functions for the thermal conducvity $f_\lambda(t)$, defined as

$$\lambda = \int_0^\infty f_\lambda(t)\mathrm{d}t \tag{17}$$

are plotted in Fig. 12. In this figure, the contribution from the translational motion and that from the rotational one are compared and their temperature dependences are also compared. From this figure we can see the cancellation in the rotational part in the integration of the correlation function. This cancellation is more complete at $T=0.194$ ε_0/k_B than at $T=0.236$ ε_0/k_B. This is the reason for the increase of the rotational contribution when the temperature is increased from $T=0.194$ ε_0/k_B to $T=0.236$ ε_0/k_B. Such cancellation is due to the oscillatory feature of the rotational motion at these temperatures a shon in Fig. 13. In this figure, the auto-correlation functions of the velocity are compared. The oscillatory motion converts to diffusive motion in the translational motion when the temperature is raised from 0.194 ε_0/k_B to 0.236 ε_0/k_B. However, the oscillatory character persists in the rotational motion.

We summarize the above discussion as follows: The contribution from the rotational motion is important in order to understand the origin of the anomalous temperature dependence of the thermal conductivity of liquid water. This conclusion is different from the result of the previous theory,[18] where the anomaly is attributed to the translational motion of the cavity molecule. The estimated relaxation time of the cavity molecule[18] seems too long compared with the result of the MD calculation.[28] We plan to perform more MD calculations using a more realistic model for water.

Finally, we mention the effect of low dimensionality on the dynamical properties. It is difficult to see the long time tail in the velocity autocorrelation function in our system because of the oscillatoty behaviour (see Fig. 11). The values obtained for the transport coefficients are finite. This may come from the small number of molecules in the system and also from the short time range examined.

The author would like to thank Dr. Shuichi Nosé for letting us know his work on the constant temperature MD method prior to publication. The computation was done at the Computer Center of the Institute for Molecular Science and at the Kyoto University Data Procesing Center. The present work was partially supported by a Grand-in-Aid for Scientific Research No. 60129031 from the Ministry of Education, Science and Culture and by the Kyoto University Data Processing Center.

References

1) D. Eisenberg and W. Kauzmann, "The Structure and Properties of Water," Oxford U. P., New York (1969).

2) G. S. Kell, "Water, a Comprehensive Treatise," ed by F. Franks, Plenum, New York (1972), Vol. 1, p. 363.

3) K. E. Bett and J. B. Cappi, *Nature* **207**, 620 (1965).

4) E. M. Stanley and R. C. Batten, *J. Phys. Chem.*, **73**, 1187 (1969) and the references cited herein.

5) T. DeFries and J. Jonas, *J. Chem. Phys.*, **66**, 896 (1977); *ibid.* **66**, 5393 (1977).

6) J. Kestin, H. E. Khalifa, H. Sookiazian, and W. A. Wakeham, *Ber. Bunsenges. Phys. Chem.*, **82**, 180 (1978).

7) L. A. Woolf, *J Chem Soc., Faraday Trans., 1,* **71**, 784 (1975).
8) L. A. Woolf, *J. Chem Soc., Faraday Trans., 1,* **72**, 1267 (1976).
9) D. J. Wilbur, T. DeFries, and J. Jonas, *J. Chem. Phys.,* **65**, 1783 (1976).
10) K. Krynicki, C. D. Green, and D. W. Sawyer. *Faraday Discuss. Chem. Soc.,* **66**, 199 (1978).
11) K. R. Harris and L. A. Woolf, *J. Chem. Soc., Faraday Trans., 1,* **76**, 377 (1980).
12) F. H. Stillinger and A. Rahman, *J. Chem. Phys.,* **61** 4973 (1974).
13) R. W. Impey, M. L. Klein, and I. R. McDonald, *J. Chem. Phys.,* **74**, 647 (1981).
14) G. Jancsó, P. Bopp, and K. Heinzinger. *Chem. Phys.,* **85**, 377 (1984).
15) E. McLaughlin, *Chem. Eng.,* **64**, 389 (1964).
16) "Water and Steam, Their Properties and Current Industrial Applications," Proc. 9th Intern. Conf. on Prop. of Steam, held at München, 1979, ed by J. Straub and K. Scheffler, Pergamon, Oxford (1980).
17) M. Eigen, *Z. Elektrochemie,* **56**, 176 (1952).
18) I. S. Andrianova, O. Ya. Samoilov, and I. Z. Fisher, *J. Struct. Chem.,* **8**, 736 (1967).
19) D. Levesque, L. Verlet, and J. Kurkijarvi, *Phys. Rev.,* **A7**, 1690 (1973).
20) W. T. Ashurst and W. G. Hoover, *Phys Rev.,* **A11** 658 (1975); J. Vermesse and D. Levesque, *Phys. Rev.,* **A19**, 1801 (1979); W. G. Hoover, D. J. Evans, R. B. Hickman, A. J. C. Ladd, W. T. Ashurst, and B. Moran, *Phys. Rev.,* **A22**, 1690 (1980).
21) D. M. Heyes, *J. Chem. Soc., Faraday Trans., 2,* **79**, 1741 (1983).
22) G. Marechal and J.-P. Ryckaert, *Chem. Phys. Lett.,* **101**, 548 (1983).
23) K. Okazaki, S. Nosé, Y. Kataoka, and T. Yamamoto, *J. Chem. Phys.,* **75**, 5864 (1981).
24) W. G. Hoover, W. T. Ashurst, and R. J. Olness, *J. Chem. Phys.,* **60**, 4043 (1974).
25) D. J. Evans, *Phys. Rev.,* **A22**, 290 (1980).
26) T. E. Wainwright, B. J. Alder, and D. M. Gass, *Phys. Rev.,* **A4**, 233 (1971).
27) S. Toxvaerd, *Mol. Phys.,* **29**, 373 (1975).
28) Y. Kataoka, *Bull. Chem. Soc. Jpn.,* **57**, 1522 (1984).
29) L. V. Woodcock, *Chem. Phys. Lett.,* **10**, 257 (1971).
30) Y. Hiwatari, E. Stoll, and T. Schneider, *J. Chem. Phys.,* **68** 3401 (1978).
31) H. C. Andersen, *J. Chem. Phys.* **72**, 2384 (1980).
32) W. G. Hoover, A. J. C. Ladd, and B. Moran, *Phys. Rev. Lett.,* **48**, 1818 (1982); D. J. Evans, *J. Chem. Phys.,* **78**, 3297 (1983).
33) H. Tanaka, K. Nakanishi, and N. Watanabe, *J. Chem. Phys.,* **78**, 2626 (1983).
34) S. Nosé *Mol. Phys.,* **52**, 255 (1984); *J. Chem. Phys.,* **81**, 511 (1984).
35) See e.g. A. Ben-Naim, "Water and Aqueous Solutions," Plenum, New York (1974).
36) R. Zwanzig, *Ann. Rev. Phys. Chem.,* **16**, 67 (1965); R. Kubo, in Ref. 16, p. 303.
37) C. W. Gear, "Numerical Initial Value Problems in Ordinary Differential Equations," Prentice-Hall, Princeton (1971).
38) J. Kushick and B. J. Berne, "Statistical Mechanics, Part B: Time-Dependent Processes," ed by B. J. Berne, Plenum, New York (1967), p. 41.
39) H. Kanno and C. A. Angell, *J. Chem. Phys.,* **73**, 1940 (1980).
40) J. Kestin, J. V, Sengers. B. Kamgar-Parsi, and J. M. H. Levelt Sengers, *J. Phy. Chem. Ref. Data,* **13**, 175 (1984).
41) H. Kanno and C. A. Angell, *J. Chem. Phys.,* **70**, 4008 (1979).
42) C. A. Angell, M Oguni, and W. J. Sinchina, *J. Phys. Chem.,* **86**, 998 (1982); M. Oguni and C. A. Angell, *J. Chem. Phys.,* **73**, 1948 (1980); *ibid.,* **78**, 7334 (1983).
43) J. Rouch, C. C. Lai, and S.-H. Chen, *J. Chem. Phys.,* **65**, 4016, (1977); *ibid.,* **66**, 5031 (1977); J. Teixeira and J. Leblond, *J. de Phys.* **39**, L83 (1978).
44) J. Yata, T. Minamiyama, T. Kim, N. Yokogawa, and H. Murai, in Ref. 16, p. 431.